APPLIED ORGANOMETALLIC CHEMISTRY
Appl. Organometal. Chem. **13**, 245–259 (1999)

Cyclic Siloxanes and Silsesquioxanes as Cores and Frameworks for the Construction of Ferrocenyl Dendrimers and Polymers

Carmen M. Casado,[1] Isabel Cuadrado,[1]* Moisés Morán,[1] Beatriz Alonso,[1] Mario Barranco[1] and José Losada[2]
[1]Departamento de Química Inorgánica, Facultad de Ciencias, Universidad Autónoma de Madrid, Cantoblanco 28049-Madrid, Spain
[2]Escuela Técnica Superior de Ingenieros Industriales, Universidad Politécnica de Madrid, 28006-Madrid, Spain

Starting from 1,3,5,7-tetramethylcyclotetrasiloxane as core, novel ferrocenyl silicon-containing dendrimers have been constructed up to the third generation, which contains 16 peripheral ferrocene moieties. As precursors of these ferrocenyl dendritic molecules, Si—Cl- and Si—allyl-terminated cyclotetrasiloxane-based dendrimers were also built step by step, by the repetition of hydrosilylation and alkenylation reactions as growing steps. The dendritic structures have been confirmed by ^{1}H, ^{13}C and ^{29}Si NMR, infrared spectroscopy, elemental analysis, mass spectrometry and vapor-pressure osmometry. Solution electrochemical studies showed that all the ferrocenyl redox centers attached to the dendritic surface behave as independent, electronically isolated units, so that the dendrimers exchange all the electrons simultaneously at the same potential. We also describe the application of the first redox-active ferrocenyl polymer containing an octakis(dimethylsiloxy)octasilsesquioxane framework, as a mediator in the electrocatalytic oxidation of ascorbic acid. Copyright © 1999 John Wiley & Sons, Ltd.

Keywords: dendrimers; cyclosiloxanes; silsesquioxanes; ferrocene; silicon; polymers; electrochemistry; modified electrodes

1 INTRODUCTION

In recent years organometallic polymers have emerged as an important category of new materials (see, e.g., Refs 1–5). The interest in developing these materials resulted from the fact that the incorporation of transition metals into polymeric structures allows access to specialty materials with unusual and attractive characteristics including electrical, magnetic, preceramic and catalytic properties, and non-linear optical (NLO) effects. In many cases, however, conventional synthetic routes developed to prepare organometallic polymers unfortunately do not provide control over the molecular weight or over the position and orientation of the functional groups, and usually lead to materials either of low molecular weight, of low solubility or of poorly defined structure.

In contrast, dendritic macromolecules containing organometallic entities offer attractive advantages since they possess a precisely defined three-dimensional molecular architecture, and there is the potential to control their chemical constitution.[6] Dendrimers are nanosized, well defined, highly branched macromolecules emanating from a central core to a periphery that becomes more dense with increasing generation number (for recent reviews on dendrimers, see, e.g., Refs 7–12). On the basis of the well-known organotransition metal chemistry, it is clear that the incorporation of organometallic entities on the surface or within the dendritic structures represents a stimulating challenging target in both organometallics and dendrimers research[6] (Refs 13–20 give examples concerning organometallic dendrimers; see also Refs 21–28), because it provides a unique opportunity for tailoring organometallic dendrimers to achieve desirable properties for well-defined applications (for example, as dendritic catalysts, in multielec-

* Correspondence to: Isabel Cuadrado, Departamento de Química Inorgánica, Facultad de Ciencias, Universidad Autónoma de Madrid, Cantoblanco 28049-Madrid, Spain.
E-mail: isabel.cuadrado@uam.es
Contract/grant sponsor: Dirección General de Investigación Científica y Técnica; Contract/grant number: PB–97-0001.

 CCC 0268–2605/99/040245–15 $17.50

tron redox and photocatalytic processes, as molecular sensors, and so on).

With this in mind, in the last few years we have constructed several families of organometallic dendrimers prepared by surface functionalization of silicon- and amine-based dendritic structures with ferrocenyl,[21–23] cyclopentadienyl, chromium, iron and cobalt carbonyl moieties.[24,25] Some of these dendritic molecules have been used successfully in the modification of electrode surfaces,[26] as electron-transfer mediators in amperometric biosensors,[27] and also as effective guests for the formation of supramolecular complexes with β-cyclodextrin.[28]

On the other hand, as a part of our ongoing studies on silicon-containing organometallic compounds we recently reported the synthesis and electrochemical behavior of new classes of macromolecules containing ferrocenyl moieties together with linear[29] and cyclic[30] siloxanes, and cubic silsesquioxanes,[31] as frameworks.

Our aim now is to create new organometallic dendritic macromolecules using siloxane rings and cages as starting structures. Due to their specific geometry, both cyclosiloxanes and polyhedral silsesquioxanes promise to be useful as highly versatile and symmetric inorganic cores for the construction of new and interesting classes of dendrimers having controlled architectures (Further synthetic and electrochemical studies on organometallic dendrimers constructed from octakis-(hydromethylsiloxy)octasilsesquixane will be reported in the near future.). Likewise, incorporation of redox-active organometallic moieties on the periphery of such oligosiloxane rings and polyhedral frameworks will lead to molecular electron reservoirs capable of simultaneously transferring a controlled number of electrons at the same potential.

In this paper we report full details on the synthesis and redox properties of novel, well-defined, silicon-containing dendrimers, constructed around a cyclotetrasiloxane as tetradirectional core, containing four, eight and 16 ferrocenyl moieties located at the dendritic surface (part of these results were presented at conferences[32,33]). For this purpose, key cyclotetrasiloxane-based dendrimers with peripheral Si—allyl and Si—Cl reactive groups have been prepared as starting points for functionalized dendritic molecules. In addition, we also describe some applications of electrodes modified with a related hyperbranched ferrocenyl polymer derived from a cubic silsesquioxane,[31] as a mediator in the catalytic oxidation of ascorbic acid. The cyclic voltammetric response of such modified electrodes to the thiocyanate anion in aqueous medium is also described.

2 RESULTS AND DISCUSSION

2.1 Synthesis and characterization of cyclotetrasiloxane-based dendrimers

Our approach to the construction of the key starting cyclosiloxane-based dendritic molecules functionalized at their peripheries with Si—allyl and Si—Cl reactive sites is shown in Scheme 1. The divergent synthetic route starts with 1,3,5,7-tetramethylcyclotetrasiloxane (TMCTS) as a tetrafunctional core (generation 0) and approximates to the valuable methodology that has been previously used by van der Made *et al.*,[34] Zhou and Roovers,[35] Seyferth *et al.*[36] and by our own group[6,21] for the synthesis of carbosilane dendrimers, and involves the repetition of hydrosilylation and alkenylation reactions as the growing steps.

First, hydrosilylation of the four reactive Si—H sites in TMCTS with either chlorodimethylvinylsilane (monodirectional branching unit) or dichloromethylvinylsilane (two-directional branching unit), in the presence of Karstedt catalyst [bis(divinyltetramethyldisiloxane)platinum(0), in xylene; DVDS-Pt], afforded the silane dendrimers TMCTS-1-$(SiCl)_4$ (1) and TMCTS-1-$(SiCl_2)_4$ (2) with four SiCl and $SiCl_2$ groups, respectively. Growth of the branches in 2 was achieved by allylation of the four $SiCl_2$ groups with an excess of allylmagnesium bromide in diethyl ether at reflux, which allowed the synthesis of the octakisallyl-functionalized dendritic silane TMCTS-1-$(Siallyl_2)_4$ (3), which corresponds to a first-generation allyl. Subsequently, all the allyl groups in 3 were hydrosilylated with chlorodimethylsilane in order to obtain the target dendrimer TMCTS-2-$(SiCl)_8$ (4) with eight reactive SiCl end groups. The dendritic framework can be further expanded via hydrosilylation of 3 with dichloromethylsilane, to give TMCTS-2-$(SiCl_2)_8$ (5), and subsequent treatment of 5 with allylmagnesium bromide to yield TMCTS-2-$(Siallyl_2)_8$ (6). Hydrosilylation of 6 with dimethylchlorosilane resulted in the formation of the desired third-generation dendritic molecule functionalized with 16 reactive Si—Cl groups at the periphery, TMCTS-3-$(SiCl)_{16}$ (7).

In our syntheses, the hydrosilylation reactions

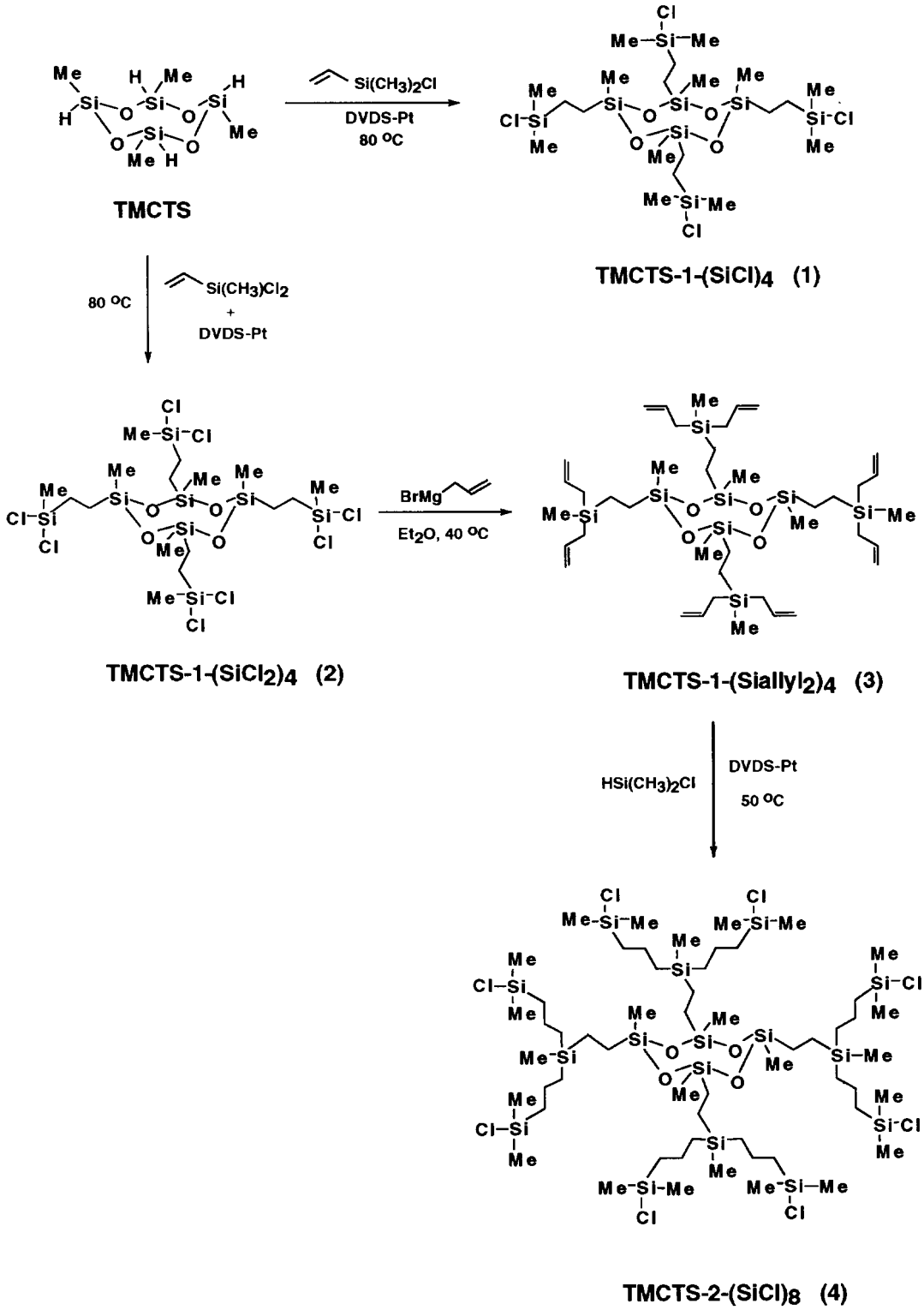

Scheme 1 Synthesis of organosilicon dendrimers from a cyclotetrasiloxane core.

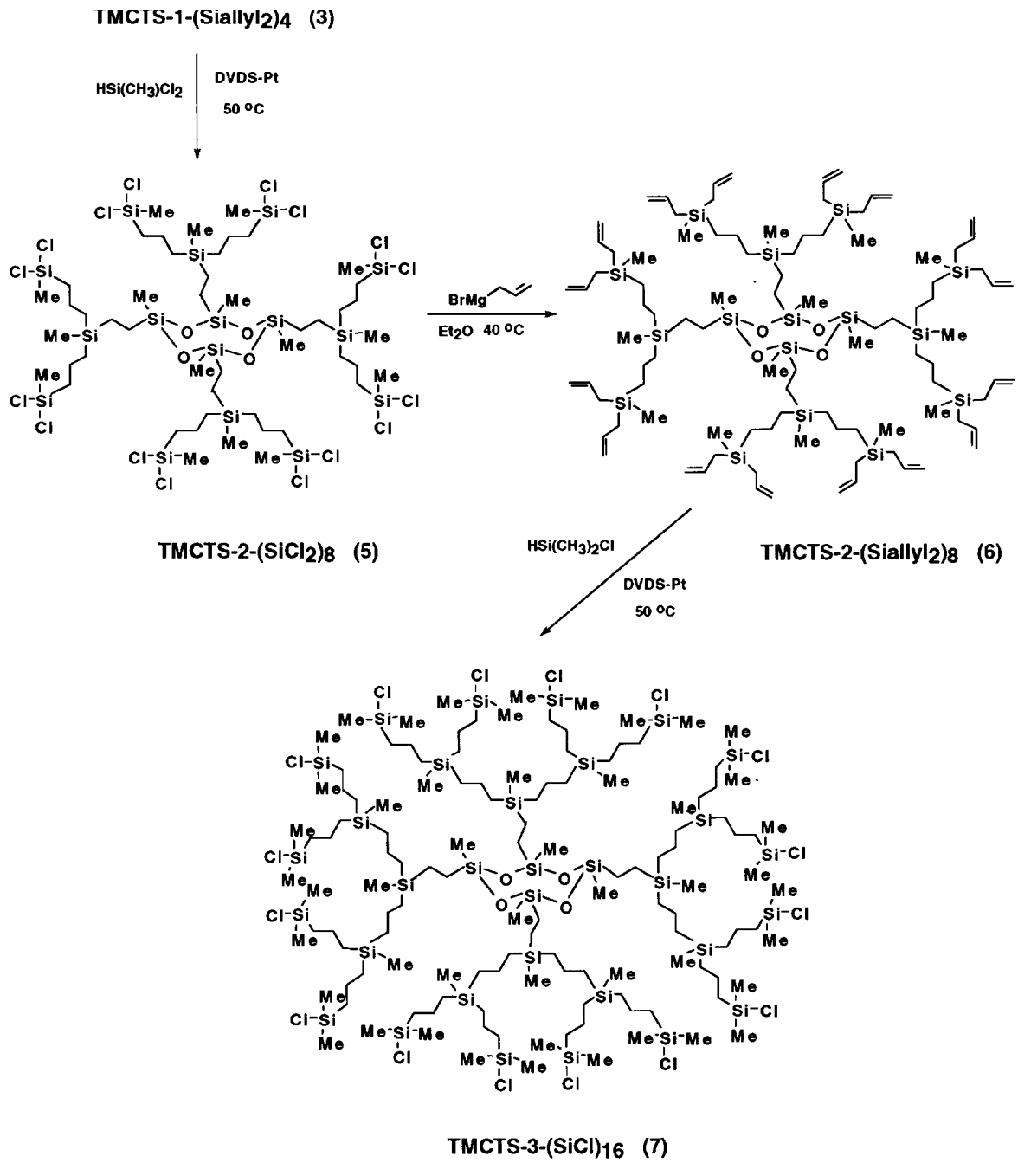

Scheme 1 Continued.

were carried out without a solvent, in the presence of Karstedt catalyst, and gave complete substitution of the Si—H or Si—allyl groups. The hydrosilylations were monitored by the disappearance of the Si—H band in the IR spectra at 2169 cm^{-1} in the synthesis of 1 and 2, and by the disappearance of the allyl band near 1630 cm^{-1} in the synthesis of 4, 5 and 7. According to the ^1H NMR spectra of the hydrosilylation products, only the β-isomers were formed, which assures a regular dendrimer growth

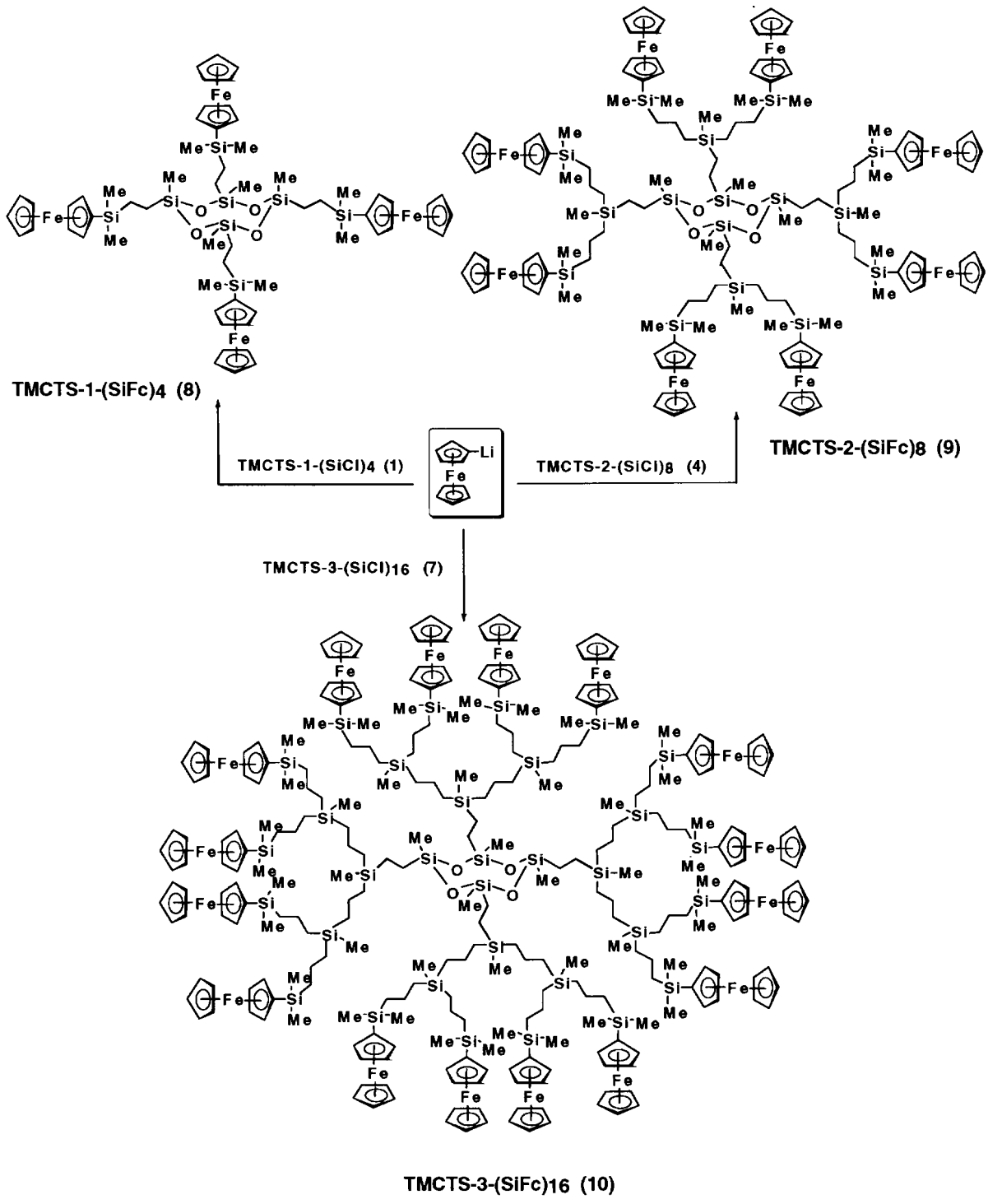

Scheme 2 Functionalization of dendrimers with ferrocenyl units.

and the generation of dendritic molecules of maximum symmetry (a critical problem in carrying out hydrosilylation of allylic groups is the occurrence of the Markovnikov addition yielding the α-isomer, which will lead to dendrimers with structural defects). All the above described reactions proceed cleanly, in nearly quantitative yields (85–95%). The new tetramethylcyclotetrasiloxane-based dendrimers are isolated as colorless or whitish viscous liquids, and display excellent solubility in common organic solvents.

The availability of the reactive Si—Cl groups located at the surface of the polyfunctionalized dendritic molecules TMCTS-1-$(SiCl)_4$, TMCTS-2-$(SiCl)_8$ and TMCTS-3-$(SiCl)_{16}$ enables the incorporation of peripheral ferrocenyl moieties in dendritic structures, via salt-elimination reaction of such Si—Cl terminated dendrimers with monolithioferrocene, FcLi (Fc = $(\eta^5\text{-}C_5H_5)Fe(\eta^5\text{-}C_5H_4)$], in THF at −15 °C (Scheme 2). These reactions afforded the first, second and third generation of dendritic molecules TMCTS-1-$(SiFc)_4$ (8), TMCTS-2-$(SiFc)_8$ (9) and TMCTS-3-$(SiFc)_{16}$ (10), possessing four, eight and 16 ferrocenyl moieties, respectively, directly bonded to the external silicon atoms of the cyclotetrasiloxane-based dendritic framework. The ferrocenyl dendrimers were carefully purified by successive column chromatographies on silica, eluting with hexane: THF mixtures, and the three ferrocenyl dendrimers were isolated as air-stable orange oils.

The identity of the novel cyclotetrasiloxane-based dendrimers was straightforwardly confirmed by a variety of techniques, including ^1H, ^{13}C and ^{29}Si NMR and IR spectroscopies and UV–visible spectroscopy, as well as by fast atom bombardment mass spectrometry (FAB–MS), molecular weight determination (VPO) and elemental analysis, which gave data consistent with their proposed structures.

The high symmetry of these macromolecules has made NMR spectroscopy a useful technique for their characterization, as only uniform growth and pure products give simple and well-defined spectra. Several spectroscopic features were characteristic of these dendritic molecules. For instance, in the ^1H NMR spectra, the different chemical shifts of the resonances corresponding to the peripheral methyl groups have been very useful in confirming the complete conversion of the terminal groups in the synthesis of the dendrimers. The methyl groups of the tetramethylcyclosiloxane core for all the different generations of dendrimers appear in the range 0–0.15 ppm. Since the Si—CH_3 signal is highly sensitive to the substituents on the silicon

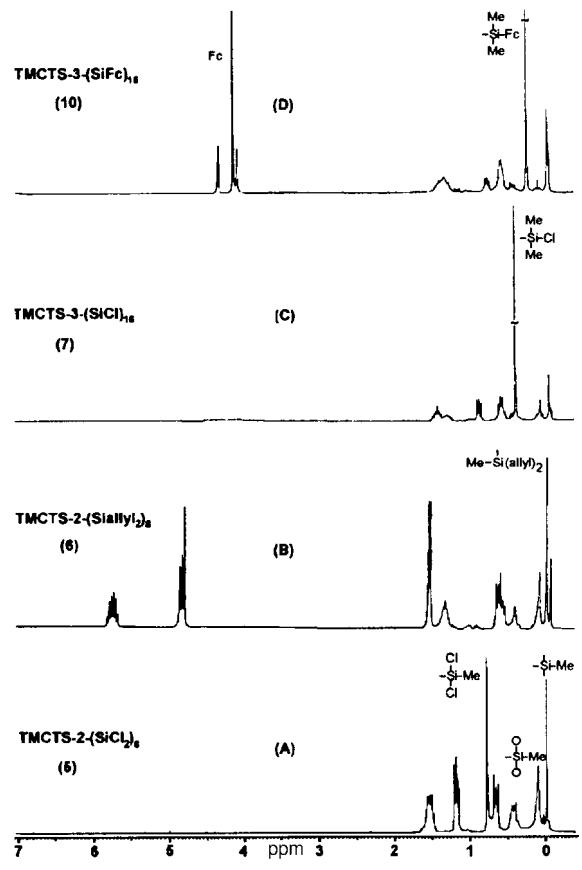

Figure 1 ^1H NMR spectra of the second and third generations of dendrimers at 360 MHz in $CDCl_3$: (A) TMCTS-2-$(SiCl_2)_8$; (B) TMCTS-2-$(Siallyl_2)_8$; (C) TMCTS-3-$(SiCl)_{16}$; and (D) TMCTS-3-$(SiFc)_{16}$.

atom, the rest of the methyl groups in the dendrimer are shifted over a broader range. For example, the substitution of the $SiCl_2$ groups in dendrimers TMCTS-*n*-$(SiCl_2)_x$ (2 and 5; Fig. 1A), for the $Si(allyl)_2$ functionalities, to obtain dendrimers TMCTS-*n*-$(Siallyl_2)_x$ (3 and 6; Figure 1B) results in a shielding of the peripheral Si—CH_3 groups (0.78 ppm in 2 and 5 to −0.01 in 3 and −0.07 ppm in 6). Conversely, a deshielding of the methyl group is observed when the $Si(allyl)_2$ groups are transformed into Si—Cl functionalities to give dendrimers TMCTS-*n*-$(SiCl)_x$ (1, 4 and 7; Figure 1C), in which the Si—CH_3 singlet appears at 0.4 ppm. Again, a shielding of the methyl groups (0.22 ppm) is observed when the complete functionalization of all the peripheral Si—Cl groups with ferrocenyl moieties is achieved to afford dendrimers TMCTS-*n*-$(SiFc)_x$, (8, 9 and 10; Fig. 1D). Further evidence

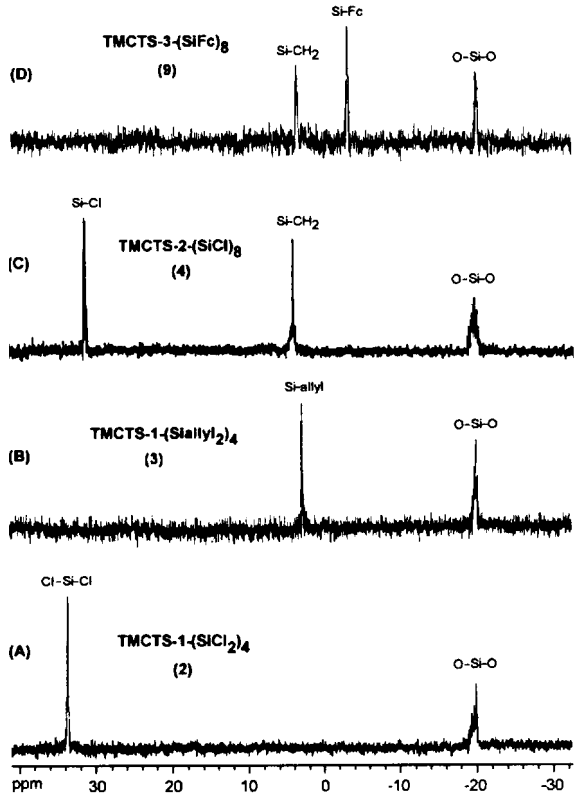

Figure 2 $^{29}Si\{^{1}H\}$ NMR spectra of the first and second generations of octafunctionalized dendrimers at 59.3 MHz in $CDCl_3$: (A) TMCTS-1-$(SiCl_2)_4$; (B) TMCTS-1-$(Siallyl_2)_4$; (C) TMCTS-2-$(SiCl)_8$; (D) TMCTS-2-$(SiFc)_8$.

for the complete functionalization of the four, eight and 16 reactive sites in the organosilicon dendritic cores with ferrocenyl moieties is provided by the expected integration of protons corresponding to the peripheral ferrocenyl groups (which appear in the range 4.06–4.32 ppm), the internal CH_2 groups of the branches and the internal methyl groups of the cyclosiloxane core moiety.

The ^{13}C NMR spectra provided further support for the structural assignments. Each of the observed spectral resonances was found to agree with the different carbon atoms present in the dendritic molecules.

Products from each step of the dendrimer synthesis were also analyzed by ^{29}Si NMR spectroscopy, which shows in all cases clearly separated signals for the different types of silicon atoms in the molecules (see for example Fig. 2). Thus, the signal for the silicon atom of the cyclotetrasiloxane core is distinguishable up to the third generation of dendrimer growth and appears in all cases far upfield at approximately −20 ppm (the commercial starting core 1,3,5,7-tetramethylcyclotetrasiloxane consists of a mixture of isomers, and as expected, the occurrence of various isomers is observable in the NMR spectra of the new dendrimers; for example, in the ^{29}Si spectra shown in Fig. 2 the broad signal at −20 ppm is indicative of the presence of various isomers) which is within the range expected for a D-type silicon atom (in siloxane chemistry the symbol D is used to represent framework silicon atoms which possess two organyl substituents, O −Si(R)(R′) −O) in a cyclic tetrasiloxane.[37] On the other hand, the outermost SiCl and $SiCl_2$ silicon atoms for dendrimers TMCTS-*n*-$(SiCl)_x$ (1, 4 and 7), and TMCTS-*n*-$(SiCl_2)_x$ (2 and 5), resonate at about 32 ppm (see for example Fig. 2A and 2C), far downfield of the Si—allyl silicon atoms which appear at 2.74 and 0.25 ppm in 3 (Fig. 2B) and 6 respectively and also of the Si—Fc silicon atom resonances shown at −0.5, −3.06, and −2.72 ppm for TMCTS-*n*-$(SiFc)_x$ (8, 9, and 10 respectively; Fig. 2D).

Not unexpectedly, only the first and second generation of ferrocenyl dendrimers 8 and 9 were found to be amenable to mass-spectral characterization. In this way, the full incorporation of four or eight ferrocenyl units, respectively, onto the dendritic surface of the dendrimers was confirmed by fast atom bombardment (FAB) mass spectra which show the molecular ion M^+, at *m/z* 1320 for 8, and at *m/z* 2804 for 9, together with some informative peaks assignable to logical fragmentation products. The dendrimer with 16 peripheral ferrocenyl moieties has a mass too high to be detected by FAB or electron impact (EI) and thus only fragmentation peaks were observed in the FAB mass spectrum. However, the molecular weight of 10 could be determined by vapor pressure osmometry (VPO), and was found to be 5695, which is similar to that expected for the proposed structure.

Evidence for the formation of the ferrocenyl dendrimers was also provided by UV–visible spectroscopy. For all three dendrimers TMCTS-*n*-$(SiFc)_x$ (8, 9 and 10), the UV–visible spectra (in CH_2Cl_2) in the region 250–800 nm showed absorptions corresponding to spin-allowed *d–d* transitions: one at 325 nm, which has been assigned to the $^1A_{1g} \rightarrow b^1E_{1g}$ transition, and a band at 447 nm assigned to overlapping $^1A_{1g} \rightarrow a^1E_{2g}$ and $^1A_{1g} \rightarrow {}^1E_{1g}$ electronic transitions.[38] In addition, the most intense bands consist of UV absorptions at 235 and

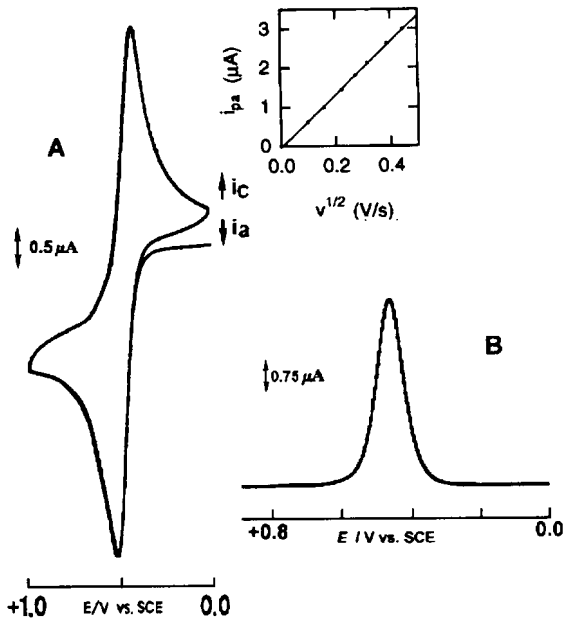

Figure 3 (A) Cyclic voltammogram (at 100 mV s^{-1}) and (B) differential pulse voltammogram of the ferrocenyl dendrimer TMCTS-3-$(SiFc)_{16}$ in a solution of CH_2Cl_2/0.1 M Bu_4NPF_6.

280 nm which correspond to ligand-to-metal charge-transfer (LMCT) transitions. These UV–visible spectra were found to be similar to those of related ferrocenyl dendrimers constructed from tetra-allylsilane as the core molecule,[22] and they are also in agreement with those found for ferrocene derivatives with organosilicon groups attached to the cyclopentadienyl rings.[39,40]

2.2 Electrochemical behavior of the cyclotetrasiloxane-based ferrocenyl dendrimers

The redox behavior of the peripherally functionalized ferrocenyl cyclosiloxane-based dendritic molecules has been studied in CH_2Cl_2 solutions containing 0.1 M tetrabutylammonium hexafluorophosphate (Bu_4NPF_6) as supporting electrolyte.

The cyclic voltammograms (CVs) of 8, 9 and 10 show a single reversible oxidation process (Fig. 3A). For the three ferrocenyl dendrimers, the peak current is linearly proportional to the square root of the scan rate *v*, indicating diffusion-controlled redox processes. Likewise, the ratio of the cathodic to anodic current (i_{pc}/i_{pa}) is essentially equal to unity, E_p is independent of the scan rate, and the peak potential separation (ΔE_p) is about 60–70 mV.

Table 1. Cyclic voltammetric data of dendrimers TMCTS-n-$(SiFc)_x$ in CH_2Cl_2 solution.

Dendrimer	E° (V)	ΔE_p (mV)	D_o (cm^2 s^{-1})[a]
TMCTS-1-$(SiFc)_4$	0.47	70	1.8×10^{-6}
TMCTS-2-$(SiFc)_8$	0.45	70	5.5×10^{-8}
TMCTS-3-$(SiFc)_{16}$	0.44	60	1.5×10^{-9}

[a] D_0 for ferrocene in CH_2Cl_2/0.1 M $Bu_4NPF_6 = 2.3 \times 10^{-5}$ cm^2 s^{-1}.

These voltammetric features clearly show that the oxidation of the dendrimers TMCTS-*n*-$(SiFc)_x$ (n = 1–3; $x = 4, 8, 16$) is chemically and electrochemically reversible, and results in the production of stable and soluble dendritic polycations. Interestingly, this result contrasts with that observed in our recent electrochemical studies on a related family of ferrocenyl-functionalized dendrimers, constructed from poly(propylenimine) dendritic cores, which undergo oxidative precipitation effects onto the electrode surfaces.[22]

The number of electrons transferred in the redox processes was estimated by coulometry after the complete oxidation of the three ferrocenyl dendrimers TMCTS-*n*-$(SiFc)_x$, carried out in CH_2Cl_2 solutions at an E_{appl} that was approximately 100 mV more positive than the respective anodic potentials (Platinum mesh, ambient temperature). The results indicated the removal of four (for 8), eight (for 9) and 15.7 (for 10) electrons/molecule.

The formal potential values E^0 for TMCTS-*n*-$(SiFc)_x$ are indicated in Table 1 and show that in going from the first to the second and third generation of dendrimers, the oxidation of the four, eight and 16 peripheral ferrocenyl moieties, respectively, occurs at essentially the same potential. This clearly suggests that the electronic environment surrounding the ferrocenes attached to the dendritic surface is independent of the dendrimer generation.

Differential pulse voltammetry (DPV) measurements gave only one wave (see for example Fig. 3B), indicating that the oxidation of the four, eight, and 16 peripheral ferrocenyl moieties occurs at the same potential.

On the other hand, the diffusion coefficients D_0 for the three ferrocenyl dendrimers in CH_2Cl_2 solution have been calculated from cyclic voltammetry using the Randles–Sevcik equation[41], and the results are listed in Table 1. As would be expected, the diffusion coefficients of our dendritic molecules are much lower than that of a small organometallic monomer of small size such as ferrocene. For

instance, for the third-generation ferrocenyl dendrimer D_0 is 1.5×10^{-9} cm^2 s^{-1}, compared with that of ferrocene which is $D_0 = 2.3 \times 10^{-5}$ cm^2 s^{-1}. Furthermore, the values of the diffusion coefficients increase as the number of peripheral ferrocenyl moieties increases; that is, D_0 increases with increasing of generation dendrimer.

The electrochemical results of CV, DPV and bulk coulometry presented here demonstrate unequivocally that in the three polyferrocenyl dendrimers the observed reversible oxidation waves represent a simultaneous multielectron transfer of four, eight and 16 electrons, respectively, as expected for independent, reversible, one-electron processes, at the same potential, of the four (in 8), eight (in 9) and 16 (in 10) non-interacting ferrocenyl redox centers.[42]

These results are in agreement with the information about the structural features of these macromolecules obtained from computer-generated molecular models performed on TMCTS-*n*-(SiFc)$_x$ (8, 9 and 10), which show that the distance between neighboring iron centers is approximately 8 Å. Consequently, the redox-active ferrocenyl moieties are separated considerably from each other so that electronic interactions between the iron centers are hindered. It is noteworthy that this result contrasts dramatically with the situation found in related ferrocenyl silicon-containing dendrimers that we have recently constructed using a convergent approach, in which the ferrocenyl moieties are in close proximity to one another in the dendritic structure, linked together by a bridging silicon atom.[23] This permits electronic communication between the metal centers, resulting in dendrimers with a different electrochemical behavior, in which the electron transfer takes place in two separate redox processes.

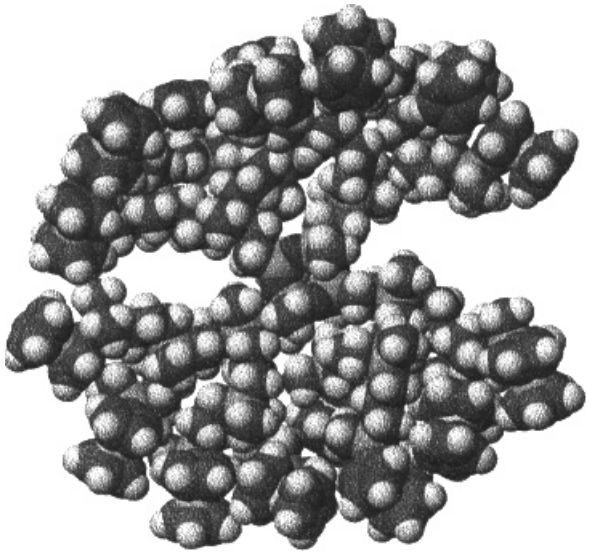

Figure 4 Structure of dendrimer TMCTS-3-(SiFc)$_{16}$ from molecular modeling.

Figure 4 illustrates the energy-minimized structure determined from CAChe™ molecular mechanics calculations of the ferrocenyl dendrimer containing 16 ferrocenyl moieties attached to the dendritic surface. From these studies we have measured approximate diameters of 2, 3 and 4 nm for the first, second and third generation of cyclotetrasiloxane-based ferrocenyl dendrimers, respectively. These values are consistent with the observed increase in the diffusion coefficients D_0 with increasing dendrimer generation.

3 ELECTROCHEMICAL APPLICATIONS OF A HYPERBRANCHED FERROCENYL POLYMER CONSTRUCTED FROM A CUBIC SILSESQUIOXANE

We have extended our preparations to more complex, highly branched, polymeric structures by assembling a polyhedral octasilsesquioxane through a suitable difunctional organometallic monomer. This involved the preparation of the three-dimensional organometallic network 11 shown in Scheme 3.[31] The synthesis of this polymer was achieved by platinum-catalyzed hydrosilylation of 1,1′-divinylferrocene with octakis(hydrodimethylsiloxy)octasilsesquioxane in toluene. The completeness of the hydrosilylation reaction and the total occupation of all the SiH terminal functions of the cubic silsesquioxane backbone are noteworthy, and were confirmed by the total absence of the SiH resonance near 5 ppm in the ^{1}H NMR spectrum of polymer 11. Solution electrochemical behavior of the ferrocenyl polymer in CH_2Cl_2/Bu_4NPF_6 solution shows a single anodic reversible wave at $E^o = 0.43$ V *vs* SCE, indicating that all the ferrocenyl centers of the polymer are independent and electrochemically equivalent.

Without doubt, the most notable aspect of the redox behavior of the octasilsesquioxane-containing ferrocenyl polymer is its ability to modify electrode surfaces. In fact, for polymer 11 an increase in the peak current upon scanning in CH_2Cl_2 was observed in the cyclic voltammograms, which indicates that the formation of an

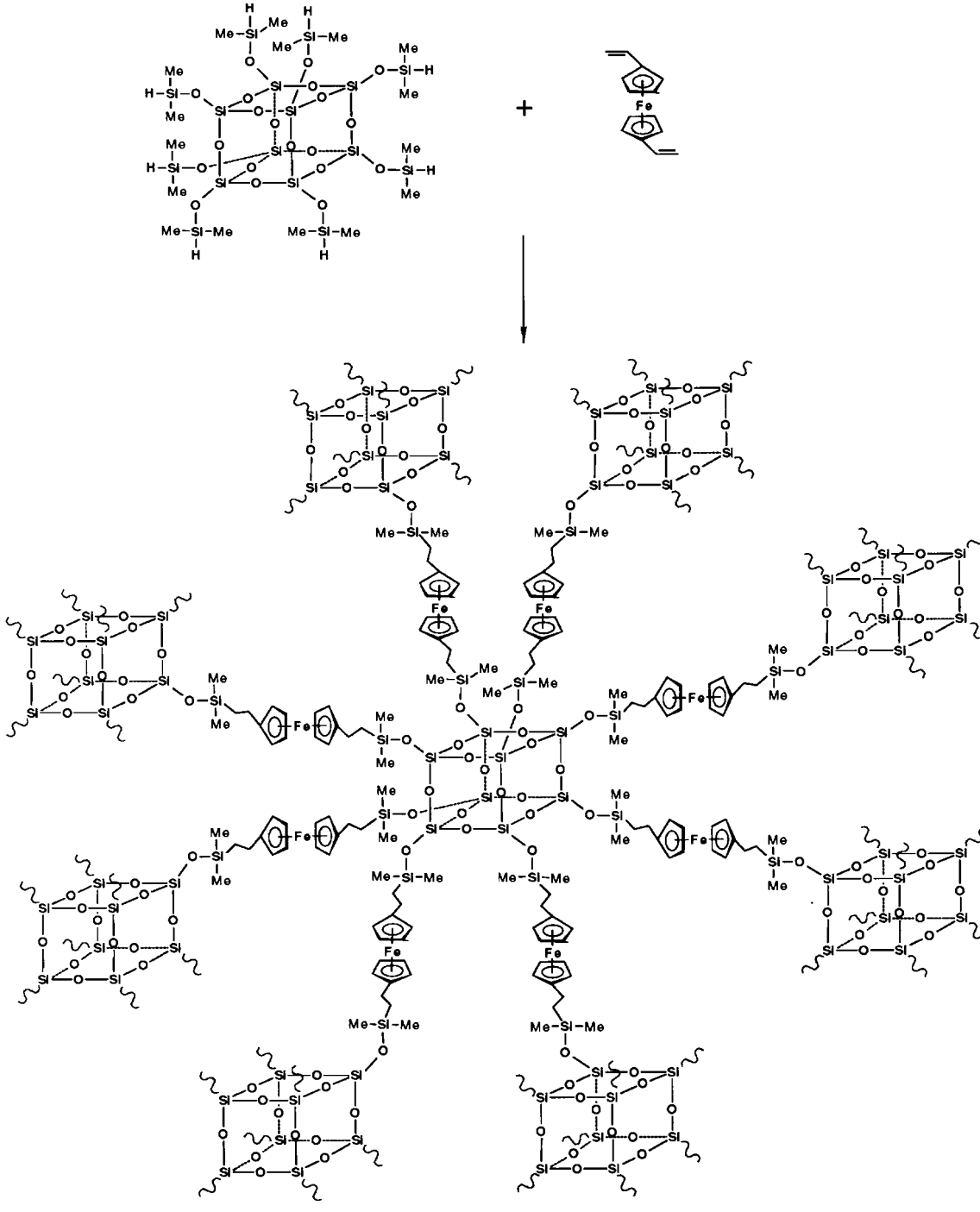

Polymer 11

Scheme 3 Ferrocenyl networks built from a cubic silsesquioxane.

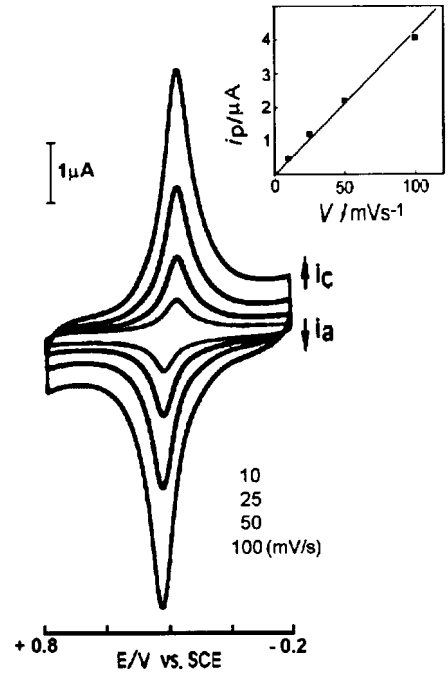

Figure 5 Cyclic voltammogram of a glassy-carbon electrode modified with a film of polymer 11, measured in 0.5 M acetic acid solution with 0.1 M $LiClO_4$.

electroactive ferrocenyl polymer film occurs on the electrode surface. Thus, platinum, gold and glassy-carbon electrode surfaces have been successfully modified with films of the silsesquioxane-based ferrocenyl polymer, resulting in detectable electroactive material persistently attached to the electrode surfaces.

Glassy-carbon electrodes were modified with films of polymer 11 by repeated cycling (in CH_2Cl_2 with either Bu_4NPF_6 or Bu_4NClO_4) between 0 and +1 V *vs* SCE, so that the amount of electroactive material electrodeposited was controlled with the number of scans. The voltammetric response of an electrodeposited film of the polymer 11 in aqueous solution (0.5 M acetic acid, 0.1 M $LiClO_4$) is shown in Fig. 5. A well-defined, symmetrical oxidation–reduction wave is observed, which is characteristic of surface-immobilized reversible redox couples, with the expected linear relationship of peak current to potential sweep rate v.[43,44] The peak-to-peak separation values (ΔE_p) are 30 mV at 10 mV s^{-1} and 40 mV at a scan rate of 50 mV s^{-1}. A formal potential value of $E^o_{surf} = +0.32$ V *vs* SCE was found for the surface-confined ferrocenyl polymer 11. These voltammetric features indicate the surface-confined nature of the electroactive ferrocenyl moieties in the dendrimer. The surface coverage, Γ (mol cm^{-2}), of electroactive ferrocenyl sites in the polymer film was determined from the integrated charge of the cyclic voltammetric wave, resulting in a value of 8.9×10^{-7} mol Fc cm^{-2}.

One remarkable feature of electrodes modified with films of this octasilsesquioxane-based ferrocenyl polymer is that they are extremely stable and reproducible. Indeed, cyclic voltammetric scans can be carried out hundreds of times in either organic or aqueous electrolyte solutions, with no loss of electroactivity. The electroactivity of the dendrimer-modified electrodes was retained after storage in air for several weeks after preparation.

One of the most important properties of chemically modified electrodes is their potential ability to mediate the electrolysis of solutes whose oxidation or reduction occurs only slowly at the corresponding bare electrode surfaces. For this reason we decided to examine the ability of the electrodes modified with films of the ferrocenyl octasilsesquioxane-based polymer to catalyze ascorbic acid

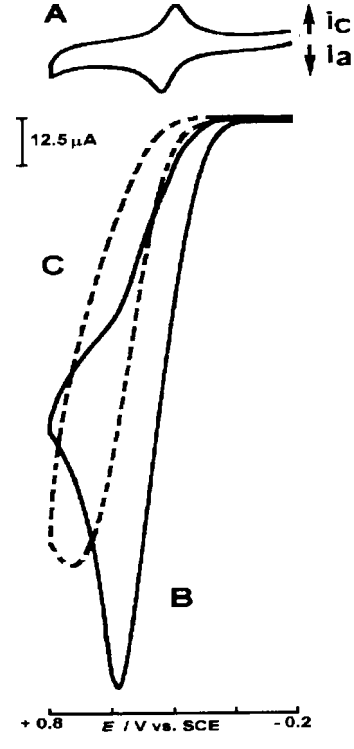

Figure 6 Cyclic voltammogram in 0.1 M acetate buffer + 0.1 M $LiClO_4$ of: (A) a glassy-carbon electrode modified with polymer 11; (B) the same electrode as in A with 10^{-3} M ascorbic acid; (C) a bare glassy-carbon electrode in 10^{-3} M ascorbic acid.

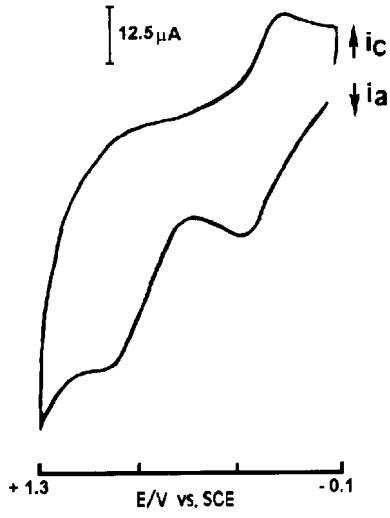

Figure 7 Cyclic voltammogram of a glassy-carbon electrode modified with a film of polymer 11 after exchange with thiocyanate from 10^{-3} M thiocyanate solution for 15 min, recorded in 0.1 M $LiClO_4$, scan rate 100 mV s^{-1}.

oxidation. The results displayed in Fig. 6 indicate that electrodes modified with films of 11 are effective in the electrocatalytic oxidation of ascorbic acid. The curve A represents the voltammetric response at a platinum electrode modified with a film of 11 in 0.1 M acetic buffer. The curve B represents the voltammetric response of the ascorbic acid (10^{-3} M) in 0.1 M acetic buffer at the same modified electrode. It can be observed that the anodic peak current of the ferrocenyl polymer film is greatly enhanced while the corresponding cathodic wave disappears, which is consistent with a catalytic process. Catalytic activity of the ferrocenyl polymer modified electrode is confirmed by the decrease in the oxidation potential (225 mV) and by the increase of the anodic peak current relative to the oxidation of the ascorbic acid at a bare electrode in the same medium (curve C).

On the other hand, when a glassy-carbon electrode modified with an oxidized film of polymer 11^{+} ClO_4^{-} is inmersed in a solution containing thiocyanate, anion exchange takes place and the SCN^{-} anions are incorporated instead of the ClO_4^{-} anions in the structure of the film. The cyclic voltammogram of the film after inmersion in 10^{-3} M thiocyanate solution for 15 min showed an oxidation peak at +0.95 V, corresponding to the thiocyanate (Fig. 7). Similar results have been obtained with CN^{-} and I^{-}. This suggests that the electrochemical properties of these ferrocenyl-modified electrodes are sensitive to the anion composition of the solutes. This can be an advantage for the electroanalysis of anions.

4 EXPERIMENTAL

4.1 General data

All reactions and subsequent manipulations were carried out under an argon atmosphere by using conventional Schlenk techniques. Solvents were purified by distillation from appropriate drying agents[45] under an atmosphere of dry argon. 1,3,5,7-Tetramethylcyclotetrasiloxane, vinyldimethylchlorosilane and vinylmethyldichlorosilane were purchased from Petrarch Systems Inc. and used as received. Chlorodimethylsilane and dichloromethylsilane (Aldrich) were distilled prior to use. *t*-Butyllithium (1.7 M and 1.5 M solutions in pentane) and allylmagnesium bromide (1.0 M solution in Et_2O) were purchased from Aldrich and used as received. Platinum–divinyltetramethyldisiloxane complex (3–3.5% in xylene) (Karstedt's catalyst), available from Fluorochem Ltd, and ferrocene (Pluto) were also used as received. Silica gel and silanized silica gel 60 (70–230 mesh) (Merck) were used for column chromatographic purifications.

Molecular mechanics calculations were made (MM2 force field) using the Cache software package (version 3.8). Models were generated using steepest descent or conjugate gradient optimization techniques, either by successive generations or by dendrons. The conformation with minimized energy was obtained from the optimized molecule using the sequential search option in the software package.

4.2 Electrochemical measurements

Cyclic voltammograms were recorded on a BAS-CV-27 potentiostat, with a platinum disk as the working electrode. In general the concentration of the solutions of the dendritic molecules were in the range 10^{-4} – 10^{-3} M, and 0.1 M $[Bu_4N][PF_6]$ was used as supporting electrolyte. Coulometric measurements were made with a PAR-379 digital coulometer, using a platinum gauze as working electrode. Differential pulse voltammograms (DPVs) were recorded by a Polarecord-E-506 Metrom, with a scan rate of 10 mV s^{-1}, a pulse

height of 20 mV and a duration of 60 ms, using CH_2Cl_2 solutions of the ferrocenyl dendrimers.

4.3 Synthesis of dendrimers

TMCTS-1-(SiCl)$_4$ (1)
To a 100-mL two-necked round-bottomed flask equipped with a reflux condenser, argon inlet and magnetic stir bar, 5.50 g (45.58 mmol) of vinyldimethylchlorosilane and 40 μl of a solution of Karstedt's catalyst (3–5% Pt) in xylene were added. After 15 min, 1 g (4.15 mmol) of 1,3,5,7-tetramethylcyclotetrasiloxane was added. The reaction mixture was heated slowly to 80 °C and stirred for 24 h. After the complete disappearance of the Si—H protons (confirmed by IR and ^{1}H NMR spectroscopies), the excess of vinyldimethylchlorosilane was removed under vacuum to afford the dendrimer 1 as a pure, whitish, viscous liquid, which was used immediately in the next reaction step. Yield: 2.85 g (95%). ^{1}H NMR ($CDCl_3$): δ 0.76 (m, 8H, CH_2SiCl), 0.53 (m, 8H, OSiCH_2), 0.40 (s, 24H, CH_3SiCl), 0.11 (s, 12H, OSiCH_3). ^{13}C{^{1}H} NMR ($CDCl_3$): δ 10.55 (*C*H_2SiCl), 8.37 (OSi*C*H_2), 0.89 (*C*H_3SiCl), −1.51 (OSi*C*H_3). ^{29}Si{^{1}H} NMR ($CDCl_3$): δ 33.13 (*Si*Cl), −19.96 (O*Si*O).

TMCTS-1-(SiCl$_2$)$_4$ (2)
This dendrimer was prepared by the same procedure as that described for 1, starting from 21.2 g (147.2 mmol) of vinylmethyldichlorosilane and 5.29 g (22 mmol) of 1,3,5,7-tetramethylcyclotetrasiloxane. Compound 2 was isolated as a whitish, viscous fluid. Yield: 16.82 g (94%). ^{1}H NMR ($CDCl_3$): δ 1.05 (m, 8H, CH_2SiCl), 0.78 (s, 12H, CH_3SiCl), 0.65 (m, 8H, OSiCH_2), 0.15 (s, 12H, OSiCH_3). ^{13}C{^{1}H} NMR ($CDCl_3$): δ 13.59 (*C*H_2SiCl), 7.96 (OSi*C*H_2), 4.29 (*C*H_3SiCl), −1.46 (OSi*C*H_3). ^{29}Si{^{1}H} NMR ($CDCl_3$): δ 33.66 (*Si*Cl), −20.10 (O*Si*O).

TMCTS-1-(Siallyl$_2$)$_4$ (3)
The reaction was carried out in a 1-l round-bottomed three-necked flask equipped with a magnetic stirrer, condenser and addition funnel. Under an inert atmosphere, the apparatus was charged with 50 ml of diethyl ether and 28.04 g (193 mmol) of allylmagnesium bromide. A solution of 16.82 g (20.90 mmol) of recently prepared 2 was added dropwise over a period of 2 h. After the addition, the mixture was refluxed at 40 °C for 12 h, cooled to 0 °C, and next hydrolyzed with saturated aqueous NH_4Cl. The organic layer was then separated from the aqueous layer, washed with water and dried over anhydrous $MgSO_4$. The solvent was removed under vacuum and the oily residue was dissolved in hexane and subjected to filtration through a pad of silanized silica. Solvent removal afforded the dendrimer 3 as a colorless viscous oil. Yield: 15.63 g (88%). ^{1}H NMR ($CDCl_3$): δ 5.76 (m, 8H, CH_2CH=CH_2), 4.83 (m, 16H, CH_2CH=CH_2), 1.56 (m, 16H, CH_2CH=CH_2), 0.47 (m, 16H, CH_2CH_2), 0.09 (s, 12H, OSiCH_3), −0.01 [s, 12H, CH_3Si(allyl)]. ^{13}C{^{1}H} NMR ($CDCl_3$): δ 134.64 (CH_2*C*H=CH_2), 113.02 (CH_2CH=*C*H_2), 20.79 (*C*H_2CH=CH_2), 8.90, 4.14 (*C*H_2*C*H_2), −1.51 (OSi*C*H_3), −6.40 [*C*H_3Si(allyl)]. ^{29}Si{^{1}H} NMR ($CDCl_3$): δ 2.74 (*Si*(allyl)), −20.05 (O*Si*O). Analysis: Calcd for $Si_8O_4C_{40}H_{80}$: C, 56.54; H,9.49. Found: C, 56.18; H, 9.50.

TMCTS-2-(SiCl)$_8$ (4)
The reaction was performed as described above for 1 and 2, starting from 1.8 g (2.12 mmol) of 3 and 3.40 g (36 mmol) of dimethylchlorosilane. Compound 4 was obtained as a yellow-to-whitish oil, which was used immediately in the next reaction step. Yield: 3.24 g (98%). ^{1}H NMR ($CDCl_3$): δ 1.44 (m, 16H, CH_2CH_2CH_2), 0.91 (m, 16H, CH_2SiCl), 0.60 (m, 16H, CH_2CH_2CH_2), 0.45 (m, 16H, SiCH_2CH_2Si), 0.39 (s, 48H, CH_3SiCl), 0.06 (s, 12H, OSiCH_3). −0.05 [s, 12H, CH_2Si(CH_3)(CH_2)$_2$]. ^{13}C{^{1}H} NMR ($CDCl_3$): δ 23.47 (CH_2*C*H_2CH_2), 17.65, 17.39 (*C*H_2CH_2*C*H_2), 9.11 4.98 (*C*H_2*C*H_2), 1.79 (*C*H_3SiCl), −1.50 (OSi*C*H_3), −5.65 [CH_2Si(*C*H_3)(CH_2)$_2$]. ^{29}Si{^{1}H} NMR ($CDCl_3$): δ 31.17 (*Si*Cl), 3.85 (*Si*(CH_2)$_3$$CH_3$], −20.05 (O*Si*O).

TMCTS-2(SiCl$_2$)$_8$ (5)
This compound was prepared by the method outlined above. From 10.00 g (11.76 mmol) of 3 and 20.40 g (177.3 mmol) of methyldichlorosilane 5 was isolated as a yellow-to-whitish oil, which was used immediately in the next reaction step. Yield: 20.40 g (98%). ^{1}H NMR ($CDCl_3$): δ 1.54 (m, 16H, CH_2CH_2CH_2), 1.18 (m, 16H, CH_2SiCl), 0.78 (s, 24H, CH_3SiCl), 0.66 (m, 16H, CH_2CH_2CH_2), 0.39 (m, 16H, SiCH_2CH_2Si), 0.09 (s, 12H, OSiCH_3), −0.02 (s, 12H, CH_2Si(CH_3)(CH_2)$_2$). ^{13}C{^{1}H} NMR ($CDCl_3$): δ 25.83 (CH_2*C*H_2CH_2), 17.23, 16.79 (*C*$H_2$$CH_2$*C*$H_2$), 9.03, 4.77 (*C*$H_2$*C*$H_2$), 5.44 (*C*$H_3$SiCl), −1.43 (OSi*C*$H_3$), −5.76 ($CH_2$Si(*C*$H_3$)($CH_2$)$_2$). ^{29}Si{^{1}H} NMR ($CDCl_3$): δ 32.17 (*Si*Cl), 4.07 [*Si*(CH_2)$_3$$CH_3$], −19.85 (O*Si*O).

TMCTS-2-(Siallyl$_2$)$_8$ (6)
This compound was prepared by the same procedure as that described for the synthesis of 3, starting from 30.07 g (207 mmol) of allylmagnesium bromide and 20.40 g (11.52 mmol) 5. Compound 6 was isolated as a colorless, viscous oil. Yield: 18.65 g (87%). ^{1}H NMR ($CDCl_3$): δ 5.76 (m, 16H, $CH_2CH{=}CH_2$), 4.83 (m, 32H, $CH_2CH{=}CH_2$), 1.55 (m, 32H, $CH_2CH{=}CH_2$), 1.33 (m, 16H, $CH_2CH_2CH_2$), 0.59 (m, 32H, $CH_2CH_2CH_2$), 0.40 (m, 16H, CH_2CH_2), 0.07 (s, 12H, $OSiCH_3$), −0.01 (s, 12H, $CH_2Si(CH_3)(CH_2)_2$), −0.07 [s, 24H, CH_3Si(allyl)]. ^{13}C{^{1}H} NMR ($CDCl_3$): δ 134.74 ($CH_2CH{=}CH_2$), 113.01 ($CH_2CH{=}CH_2$), 21.43 ($CH_2CH{=}CH_2$), 18.2–17.9 ($CH_2CH_2CH_2$), 9.17, 4.95 (CH_2CH_2), −1.59 ($OSiCH_3$), −5.66 [$CH_2Si(CH_3)(CH_2)_2$], −5.77 [CH_3Si(allyl)]. ^{29}Si{^{1}H} NMR ($CDCl_3$): δ 0.29 [*Si*(allyl)], −3.77 [*Si*$(CH_2)_3CH_3$], −20.00 (O*Si*O). Analysis: Calcd for $Si_{16}O_4C_{96}H_{102}$: C, 61.99; H,10.40. Found: C, 61.55; H, 10.52.

TMCTS-3-(SiCl)$_{16}$ (7)
The reaction was performed by the same method as that described for the synthesis of 1, starting from 5.73 g (3.08 mmol) of 6 and 10.22 g (108 mmol) of dimethylchlorosilane.Compound 7 was obtained as a yellow-to-whitish oil. Yield: 10.09 g (97%). ^{1}H NMR ($CDCl_3$): δ 1.44 (m, 32H, $CH_2CH_2CH_2SiCl$), 1.38 (m, 16H, $SiCH_2CH_2CH_2SiCH_2$), 0.89 (m, 32H, CH_2SiCl), 0.59 (m, 64H, $SiCH_2CH_2CH_2$-$SiCH_2$), 0.40 (m, 16H, $SiCH_2CH_2Si$), 0.39 (s, 96H, CH_3SiCl), 0.06 (s, 12H, $OSiCH_3$), −0.04 [s, 24H, $CH_2Si(CH_3)(CH_2)_3SiCl$], −0.07 (s, 12H, $SiCH_2CH_2SiCH_3$). ^{13}C{^{1}H} NMR ($CDCl_3$): δ 23.52 ($CH_2CH_2CH_2SiCl$), 18.8–17.7 ($SiCH_2CH_2CH_2SiCH_2CH_2CH_2$), 9.20, 5.16 ($CH_2CH_2$), 1.86 ($CH_3SiCl$), −1.40 ($OSiCH_3$), −5.02 [$(CH_2)_3Si(CH_3)(CH_2)_3$], −5.56 [$Si(CH_2)_2$-$SiCH_3$]. ^{29}Si{^{1}H} NMR ($CDCl_3$): δ 31.11 (*Si*Cl), 1.30 [*Si*$(CH_2)_3$*Si*], −20.01 (O*Si*O).

TMCTS-1-(SiFc)$_4$ (8)
(η^5-C_5H_5)Fe(η^5-C_5H_4Li) (FcLi) was generated *in situ* via the reaction of ferrocene (8.88 g, 47.76 mmol) with 0.5 equiv of *t*-BuLi in THF over 1 h at −30 °C. This mixture is allowed to warm to −15 °C and then 2.85 g (3.98 mmol) of 1 in THF was added dropwise. After 1 h at −15 °C, the reaction mixture was slowly warmed to room temperature and stirred overnight. The solvent was removed in vacuum; the orange residue was treated with hexane and filtered to remove the lithium chloride byproduct. Hexane was removed in vacuum to leave an orange oil, which was chromatographed on a silica-gel column using hexane as eluent. A first band containing ferrocene was eluted with hexane; subsequently the major red band was eluted with *n*-hexane/THF (10:1 v/v), which after solvent removal gave the desired product as a red–orange oil. Yield: 0.58 g (32%). ^{1}H NMR ($CDCl_3$): δ 4.32, 4.12, 4.08 (m, 36H, ferrocenyl H), 0.59 (m, 8H, $CH_2SiC_5H_4$), 0.45 (m, 8H, $OSiCH_2$), 0.22 (s, 24H, $CH_3SiC_5H_4$), 0.06 (s, 12H, $OSiCH_3$). ^{13}C{^{1}H} NMR ($CDCl_3$): δ 72.99, 70.54, 68.05 (ferrocenyl C), 9.40, 8.00 (CH_2CH_2), −1.49 ($OSiCH_3$), −2.81 ($CH_3SiC_5H_4$). ^{29}Si{^{1}H} NMR ($CDCl_3$): δ −0.50 (*Si*C_5H_4), −19.65 (O*Si*O). Mass spectrum (FAB): *m/z* 1320 (M^+). Analysis: Calcd for $Si_8O_4C_{60}H_{88}Fe_4$: C, 54.54; H, 6.71. Found: C, 54.22; H, 6.82.

TMCTS-2-(SiFc)$_8$ (9)
This compound was prepared by the same method as that described for 8, starting from 9.24 g (49.68 mmol) of ferrocene and 3.24 g (2.07 mmol) of 4. Compound 9 was isolated as a red–orange oil. Yield: 1.76 g (30%). ^{1}H NMR ($CDCl_3$): δ 4.31, 4.12, 4.06 (m, 72H, ferrocenyl H), 1.38 (m, 16H, $CH_2CH_2CH_2$), 0.74 (m, 16H, $CH_2SiC_5H_4$), 0.58 (m, 16H, $CH_2CH_2CH_2$), 0.42 (m, 16H, $SiCH_2CH_2Si$), 0.22 (s, 48H, $CH_3SiC_5H_4$), 0.08 (s,12H, $OSiCH_3$) −0.05 [s, 12H, $CH_2Si(CH_3)(CH_2)_2$]. ^{13}C{^{1}H} NMR ($CDCl_3$): δ 72.90, 70.55, 68.04 (ferrocenyl C), 21.51 ($CH_2CH_2CH_2$), 18.62, 18.13 ($CH_2CH_2CH_2$), 9.26, 4.97 (CH_2CH_2), −1.49 ($OSiCH_3$), −2.05 ($CH_3SiC_5H_4$), −5.45 [$CH_2Si(CH_3)(CH_2)_2$]. ^{29}Si{^{1}H} NMR ($CDCl_3$): δ 3.65 [*Si*$(CH_2)_3CH_3$], −3.06 (*Si*C_5H_4), −20.00 (O*Si*O). Mass spectrum (FAB): *m/z* 2804 (M^+). Analysis: Calcd for $Si_{16}O_4C_{136}H_{208}Fe_8$: C, 58.27; H, 7.48. Found: C, 57.95; H, 7.64.

TMCTS-3-(SiFc)$_{16}$ (10)
The reaction was carried out as for the preparation of 8 and 9, starting from 13.33 g (71.71 mmol) of ferrocene and 5.05 g (1.50 mmol) of 7. Compound 10 was obtained as a red–orange oil. Yield: 2.40 g (28%). ^{1}H NMR ($CDCl_3$): δ 4.32, 4.12, 4.07 (m, 144H, ferrocenyl H), 1.38 (m, 48H, $CH_2CH_2CH_2$), 0.74 (m, 32H, $CH_2SiC_5H_4$), 0.56 (m, 64H, $SiCH_2CH_2CH_2SiCH_2$), 0.43 (m, 16H, $SiCH_2CH_2$-Si), 0.22 (s, 96H, $CH_3SiC_5H_4$), 0.07 (s, 12H, $OSiCH_3$), −0.05, −0.07 (s, 36H, $CH_2Si(CH_3)CH_2$). ^{13}C{^{1}H} NMR ($CDCl_3$): δ 73.33, 71.13, 68.49 (ferrocenyl C), 22.08–19 ($CH_2CH_2CH_2SiCH_2CH_2CH_2$), 9.76, 6.25 ($CH_2CH_2$), −1.50, −1.70, −3.11, −4.44 (CH_3Si).

$^{29}Si\{^{1}H\}$ NMR ($CDCl_3$): δ 1.48 [$Si(CH_2)_3Si$], −2.72 (SiC_5H_4), −20.01 ($OSiO$). Mol. wt (VPO, CH_2Cl_2): 5695, calcd 5767. Analysis: Calcd for $Si_{32}O_4C_{288}H_{448}Fe_{16}$: C, 59.98; H, 7.83. Found: C, 59.60; H, 8.01%.

Acknowledgements We thank the Dirección General de Investigación Científica y Técnica (Project No. PB–97-0001) for financial support of this research.

REFERENCES

1. Inorganic and Organometallic Polymers II. Advanced Materials and Intermediates, Wisian-Neilson, P., Allcock, H. R. and Wynne, K. J. (eds), American Chemical Society, ACS Symp. Ser. No. 572, Washington DC, 1994.
2. Inorganic and Metal-Containing Polymeric Materials, Sheats, J. E., Carraher, C. E., Jr, Pittman, C. U., Jr, Zeldin, M. and Currell, B. (eds), Plenum Press, New York, 1990.
3. Inorganic and Organometallic Polymers, Zeldin, M., Wynne, K. J. and Allcock, H. R. (eds), American Chemical Society, ACS Symp. Ser. No. 360, Washington DC, 1988.
4. H. R.Allcock, *Adv. Mater.* **6**, 106 (1994).
5. I.Manners, *Angew. Chem., Int. Ed. Engl.* **35**, 1602 (1996).
6. I. Cuadrado, M. Morán, J. Losada, C. M. Casado, C. Pascual, B. Alonso and F. Lobete, in: Advances in Dendritic Macromolecules, Vol. 3, Newkome, G. R. (ed.), JAI Press, Greenwich, CT, 1996, p. 151.
7. G. R. Newkome, C. N. Moorefield and F. Vögtle, Dendritic Molecules: Concepts, Synthesis, Perspectives, VCH, Weinheim, 1996.
8. Advances in Dendritic Macromolecules, Vols 1 and 2, Newkome, G. R. (ed.), JAI Press, Greenwich, CT, 1994 and 1995 respectively.
9. D. A. Tomalia and H. D. Durst, Topics Cur. Chem. **165**, 193 (1993).
10. J. Issberner, R. Moors and F. Vögtle, *Angew. Chem., Int. Ed. Engl.* **33**, 2413 (1994).
11. J. M. Fréchet, *Science* **263**, 1710 (1994).
12. N. Ardoin and D. Astruc, *Bull. Soc. Chim. Fr.* **132**, 875 (1995).
13. M. Bardaji, M. Kustos, A.-M. Caminade, J.-P. Majoral and B. Chaudret, *Organometallics* **16**, 403 (1997).
14. C. Valério, J.-L. Fillaut, J. Ruiz, J. Guittard, J.-C. Blais and D. Astruc, *J. Am. Chem. Soc.* **119**, 2588 (1997).
15. P. Jutzi, C. Batz, B. Neumann and H.-G. Stammler, *Angew. Chem., Int. Ed. Engl.* **35**, 2118 (1996).
16. W. T. S. Huck, F. C. J. M. van Veggel, B. L. Kropman and D. N. Reinhoudt, *Angew. Chem., Int. Ed. Engl.* **35**, 1213 (1996).
17. S. Achar, J. J. Vittal and R. J. Puddephatt, *Organometallics* **15**, 43 (1996).
18. Y. H. Liao and J. R. Moss, *Organometallics* **15**, 4307 (1996).
19. D. Seyferth, T. Kugita, A. Rheingold and G. P. A. Yap, *Organometallics* **14**, 5362 (1995).
20. J. W. J. Knapen, A. W. van der Made, J. C. de Wilde, P. W. N. M. van Leeuwen, P. Wijkens, D. Grove and G. van Koten, *Nature (London)* **372**, 659 (1994).
21. B. Alonso, I. Cuadrado, M. Morán and Losada, *J. Chem. Soc., Chem. Commun.* 2575 (1994).
22. I. Cuadrado, M. Morán, C. M. Casado, B. Alonso, F. Lobete, B. García, M. Ibisate and J. Losada, *Organometallics* **15**, 5278 (1996).
23. I. Cuadrado, C. M. Casado, B. Alonso, M. Morán and J. Losada, *J. Am. Chem. Soc.* **119**, 7613 (1997).
24. I. Cuadrado, M. Morán, A. Moya, C. M. Casado, M. Barranco and B. Alonso, *Inorg. Chim. Acta* **251**, 5 (1996).
25. F. Lobete, I. Cuadrado, C. M. Casado, B. Alonso, M. Morán and J. Losada, *J. Organomet. Chem.* **509**, 109 (1996).
26. B. Alonso, M. Morán, C.M. Casado, F. Lobete, J. Losada and I. Cuadrado, *Chem. Mater.* **7**, 1440 (1995).
27. J. Losada, I. Cuadrado, M. Morán, C. M. Casado, B. Alonso and M. Barranco, *Anal. Chim. Acta* **251**, 5 (1996).
28. R. Castro, I. Cuadrado, B. Alonso, C. M. Casado, M. Morán and A. Kaifer, *J. Am. Chem. Soc.* **119**, 5760 (1997).
29. C. M. Casado, M. Morán, J. Losada and I. Cuadrado, *Inorg. Chem.* **34**, 1668 (1995).
30. C. M. Casado, I. Cuadrado, M. Morán, B. Alonso, F. Lobete and J. Losada, *Organometallics* **14**, 2618 (1995).
31. M. Morán, C. M. Casado, I. Cuadrado and J. Losada, *Organometallics* **12**, 4327 (1993).
32. 211st American Chemical Society National Meeting, New Orleans, LA, USA, 24–28 March 1996.
33. XI International Symposium on Organosilicon Chemistry, Montpellier, France, September 1996, paper PB46.
34. A. W. van der Made and P. W. N. M. van Leeuwen, *J. Chem. Soc., Chem. Commun.* 1400 (1992).
35. L.-L. Zhou and J. Roovers, *Macromolecules* **26**, 963 (1993).
36. D. Seyferth, D. Y. Son, A. L. Rheingold and R. L. Ostrander, *Organometallics* **13**, 2682 (1994).
37. E. A. Williams, in: The Chemistry of Organic Silicon Compounds, Part 1, Patai, S. and Rappoport, Z. (eds), John Wiley, New York, 1989, p. 511.
38. Y. S. Sohn, D. N. Hendrickson and H. B. Gray, *J. Am. Chem. Soc.* **93**, 3603 (1971).
39. D. A. Foucher, R. Ziembinski, B.-Z. Tang, P. M. Macdonald, J. Massey, C. R. Jaeger, G. J. Vancso and I. Manners, *Macromolecules* **26**, 2878 (1993).
40. M. T. Nguyen, A. F. Diaz and K. H. Pannell, *Chem. Mater.* **5**, 1389 (1993).
41. A. J. Bard and L. R. Faulkner, Electrochemical Methods, Wiley, New York, 1980.
42. J. B. Flanagan, S. Margel, A. J. Bard and F. C. Anson, *J. Am. Chem. Soc.*, **100**, 4248 (1978).
43. H. D. Abruña, *Coord. Chem. Rev.*, **86**, 135 (1988).
44. R. W. Murray, in: Electroanalytical Chemistry, Vol. 13 Bard, A. J. (ed.), Dekker, New York, 1984.
45. D. D. Perrin, W. L. F. Armarego and D. R. Perrin, Purification of Laboratory Chemicals, 2nd edn, Pergamon, New York, 1988.

